Armenian Journal of Physics, 2013, vol. 6, issue 3, pp. 149-161

Study of the Light Nuclei Cluster Structures in Three-Body Photodisintegration Reactions. Application for the Excited States of ^{6}He Nucleus

N. Demekhina, H. Hakobyan, Zh. Manukyan, A. Sirunyan*, H. Vartapetian

A.I.Alikhanyan National Science Laboratory
(Yerevan Physics Institute)
**e-mail:* sirunian@mail.yerphi.am

Received 27 August 2013

We dedicate this paper to the bright memory of academician NAS RA Hamlet Vartapetian

Key words: light nuclei, cluster structure, photodisintegration

Abstract – An experimental program for the study of cluster structures of excited states in the isotopes of He, Li and Be nuclei in three-body photo-disintegration processes is proposed. The investigations will be performed with ^{6}Li, ^{7}Li and ^{9}Be targets in seven photo-disintegration reactions. As an application, the photo-disintegration of ^{7}Li nuclei into the (t+t+p) final state with excitation and decay of neutron-rich ^{6}He nucleus into the (t+t) channel is considered. The full Monte-Carlo simulation of the experiment is done with a special impact on the study of experimental setup performance, concerning the photon and excited states energy resolutions and efficiency. The experiment will be carried out at the bremsstrahlung photon beam of Yerevan Electron Synchrotron, working in stretcher mode at electron energy of 75 MeV.

1. Introduction

Clustering aspect is one of the most important ingredients of the nuclear many-body problem [1]. Owing to the recent theoretical and experimental developments, the domain of the cluster studies is rapidly expanding toward highly excited and neutron-rich nuclei having also an importance in processes of nuclear-synthesis [2-6]. The strong advance is achieved in the theoretical description of excited states of ^{12}C within condensed alphas model [2] and newest *ab initio* lattice calculations [3] supported by high quality experimental investigations worldwide [4-9]. The intensive discussions, in particular, on the α - molecules' configurations in ^{12}C and ^{16}O, renewed our interest in the clustering of the highly excited states in stable and unstable light nuclei.

It is well known that the ground and low-lying states of light nuclei possess a pronounced quasi-molecular structure, whose components are α particle and residual nuclear fragments: n, p, d, t, ^{3}He and α as well. With excitation energy increase the hierarchy of the excited structures is expected to be seen, starting from simple particle-hole (1p-1h) configuration of the shell-model, the Soft Dipole Mode resonances (SDM, IVSDM) (see [9-11] and references therein) with attribution of the observed strength to the dipole oscillation of the core alpha cluster against of valence nucleons in A=6 system [11], the cluster molecular states of rotational type for example, built on the strongly deformed cluster configuration [8], collective dipole oscillations of nucleon assembly (Giant Dipole Resonance - GDR) [12,13]. The excitation of GDR in the clusters (^{4}He, ^{4}H) of the light nuclei is also observed [14]. At energies sufficient for α-particle break-up, the primary cluster structure is changed from dominant α-clustering to a coexistence of different structures and involves the lighter fragments. This is also the threshold for GDR excitation, although it is not well collectivized and may consist of few broad structures having their own orbital symmetry and own decay modes. It would be interesting to investigate if the excited cluster molecules can coexist in the energy range of SDM or GDR excitation. There is no reliable experimental observations yet. However, it is known that decay of GDR can proceed through the compound nuclei or semi-direct reactions mechanisms and in both cases the formation of intermediate resonance states is not excluded.

It is not also obvious that the observed decay products, clusters and nucleons, fully reflect the cluster structure of the parent nuclei, as they can be formed in the final state interaction. So the exact determination of decay schemes, levels' energy, widths and spins is informative in choosing and building the adequate theoretical models.

The primary goal of this project is to investigate the excited cluster states of light nuclei in mass number range A=5-9 where the experimental data on the highly excited states study are not numerous and there is a visible inconsistency on the excited states parameters. This is in particular valid for the excited states of neutron-rich ^{6}He nuclei on the identification of energy levels and decay modes. The program of the light nuclei investigation is presented in section 2 and its particular case for the ^{6}He nuclei is discussed in section 3.

2. The program of the excited structures study

In this study (see also [22]) we consider the photo-disintegration reactions with three-body final states γ+A $\rightarrow$ 1+2+3, where the particles (1, 2, 3) are in general the nucleons (p, n) and light nuclei (d, t,^{3}He,^{4}He (α)). In these conditions we can observe the following seven photo-disintegration reactions:

List of γ + A $\rightarrow$ 1+2+3 reactions

$\gamma + {}^6\text{Li} \rightarrow t + d + p$
$\gamma + {}^6\text{Li} \rightarrow {}^3\text{He} + d + n$
$\gamma + {}^6\text{Li} \rightarrow \alpha + p + n$
$\gamma + {}^7\text{Li} \rightarrow t + t + p$
$\gamma + {}^7\text{Li} \rightarrow {}^3\text{He} + t + n$
$\gamma + {}^7\text{Li} \rightarrow \alpha + d + n$
$\gamma + {}^9\text{Be} \rightarrow \alpha + \alpha + n$

As one may see from this list, the particles (1,2) are (d, t, ^{3}He, α) for the six reactions and (p, α) for the ($\gamma + {}^6\text{Li} \rightarrow \alpha + p + n$) one.

There are few paths to the same final states formation in these reactions:

- The three channels with excitation of intermediate two-particle resonances: γ +A$\rightarrow$ (12)*+N, γ +A$\rightarrow$ (1N)*+2 and γ +A$\rightarrow$ (2N)*+1 with 3 types of excited states, $(12)^*$, $(1N)^*$ and $(2N)^*$, decaying into the final three-particle states 1+2+N. The abbreviation N means a nucleon.
- A statistical channel γ +A$\rightarrow$1+2+N which represents in general the physical background for the resonance channels and which can be calculated as a three-body phase-space.
- The reaction channels of production and decay of the 3 particles resonance $(1+2+N)^*$ states in target nuclei.

For the study of these seven reactions γ +A$\rightarrow$ 1+2+N, the production angles and the kinetic energy of two known particles (1, 2) will be measured in coincidence in two-arm setup. These measurements provide the data for complete kinematical reconstruction of three body-final state, including the kinematics of (12) resonance decay, the excitation energy (E_x) and width (Γ_x) of the excited states and energy of incident photon (E_γ).

These seven photo-disintegration reactions allow to study the 24 cluster structures of excited states in seven nuclei: ^{5}He, ^{6}He, ^{5}Li, ^{6}Li, ^{7}Li, ^{8}Be, ^{9}Be:

^{5}He $\rightarrow$ (α+n), (t+d) - targets ^{6}Li, ^{7}Li, ^{9}Be

$^6He \rightarrow (t+t)$ - target ^7Li
$^5Li \rightarrow (\alpha+p), (^3He+d)$ - target ^6Li
$^6Li \rightarrow (\alpha+d), (^3He+t)$ - target ^7Li and
$(^5Li^*+n), (^5He^*+p), (\alpha+p+n), (^3He+d+n), (t+d+p)$ - target ^6Li
$^7Li \rightarrow (^6Li^*+n), (^6He^*+p), (^5He^*+d), (\alpha+d+n), (t+n+^3He), (t+t+p)$ - target ^7Li
$^8Be \rightarrow (\alpha+\alpha), (^6Li+d), (^7Li+p)$ - target ^9Be
$^9Be \rightarrow (^8Be^*+n), (^5He^*+\alpha), (\alpha+\alpha+n)$ - target ^9Be

The study of $(12)^*$ excited states will suffer from the presence of additional background source, the intermediate resonance excitation in competitive $[(1N)^*+2]$ and $[(2N)^*+1]$ channels, which must be identified and separated from the studied process. There is one additional resonance state of $(1N)^*$ or $(2N)^*$ type for the six reactions, except the $\gamma + {}^7Li \rightarrow {}^3He + t + n$ one with excitation of three additional resonances: $^6Li^*(^3He+t)$, $^4He^*(^3He+n)$ and $^4H^*(t+n)$. For each reaction channel the most favorable kinematical conditions for the detection efficiency and low background should be identified using Monte-Carlo simulations. The decays products presented above can reveal a cosmological interest. For example decay of ^8Be nuclei to ^7Li+p, permitted at excitation energy $E_x > 17.2$MeV, can contribute directly into the primordial abundance of ^7Li isotope, while the decay to ^7Be+n and ^6Li+d ($E_x >$ 21MeV) contributes indirectly, through the charge-exchange $n+{}^7Be \rightarrow {}^7Li+p$ and neutron radiation capture $n+{}^6Li \rightarrow {}^7Li+\gamma$ reactions.

3. Application for the two-cluster (t+t) excited states of $^6He^*$ nucleus

The ^6He is a typical neutron-skin nuclei with a low separation energy (0.975 MeV) of a neutron pair located outside of α-core [20].
The last compilation data [21] on the level structure of ^6He dated by 2002 are shown in Table 1, where the observation of energy levels at 15.4, 32 and 36 MeV are under question.

Table 1.The energy levels of ^6He [21]

E_x (MeV)	J^π ,T	Γ/2(MeV)	Decay
g.s.	0+, 1	-	β−
1.8	2+, 1	0.113	α, n
5.6 ± 0.3	(2+, 1-, 0+); 1	12.1 ± 1.1	
14.6 ± 0.7	(1−, 2−); 1	7.4 ± 1.0	
15.5 ± 0.5		4 ± 2	
23.3 ± 1.0		14.8 ± 2.3	
32		≤ 2	
36		≤ 2	

For the experimental study of ^6He excited states decay into the (tt) channel, the nucleon pick-up or break-up reactions [9-11,15-18], as well as the photodisintegration [23] and stopped π-meson absorption [19] were used.

- The most recent result on ^6He energy levels has been obtained at INR (Kiev, Ukraine) - INFN (Italy) collaboration [15] in the reaction $^3H(\alpha, tt)p$ using 67 MeV ^4He-beam and complete kinematical reconstruction of three body final state up to E_x = 20 MeV. The three statistically reliable narrow resonances with width FWHM ≈ 1 MeV at energies E_x = 14.0 ± 0.4 MeV, 16.1 ± 0.4 MeV and 18.3 ± 0.2 MeV were observed. The important achievement of this experimental work is the careful separation of competitive $^3H(\alpha,{}^4He^*,t)$ reaction with subsequent decay of excited $^4He^*$ states into t+p pair, leading finally to the same (ttp) final state. The Dalitz plot analyses were used.
- The narrow structures at E_x = 13.6, 15.4, 17.7 and 23.7 MeV [16] were observed 35 years ago in the nucleon break-up reaction $^7Li(n, d)^6He^*$ with 56.3 MeV neutron beam and inclusive deuteron

measurements. No decay mode of ^{6}He* was identified. Apart of the excited ^{6}He nuclei the other resonant states with close Q-values can be also produced: ^{4}H*+d or ^{5}He*+n, leading through decay to the four body final states.

- The statistically reliable structure at energy E_x = 14 MeV and width app. 5 MeV as well as the broad structure at 25 MeV and width app. 5-7 MeV were observed in ^{7}Li(^{6}Li, ^{7}Be)^{6}H reaction with 93 MeV ^{6}Li beam [17]. The structure at 14 MeV seems might be de-convoluted into two peaks at app. 13 and 16 MeV. The similar structures were also observed in the same reaction at beam energy 350 MeV [18].
- In kinematically complete experiment, with the beam of the stopped negative pions in the reaction ^{9}Be(π, tt)t, the three resonances at energies 15.4±0.6, 20.9±0.3 and 31.1±1.0 MeV have been observed using the Dalitz plot and invariant mass distributions analyses [19].

Comparing the results on the observed narrow structures one may confirm the agreement of Ref. [15-19] on the presence of two resonances at energies around E_x = 14 and 16 MeV taking into account the statistical uncertainties and energy resolution. The compatibility of data on the resonances at 18±0.2 MeV [15] and 20.9±0.3 MeV [19] need to be confirmed, as well as the observation of narrow resonances at energies 23.7 MeV [16] and 31 MeV [19].

There are also the recent experimental data of Osaka group (Japan) [10], with observation of low strength broad structure at 18 MeV (FWHM~7-10 MeV) in the reactions ^{7}Li(^{6}Li,^{7}Be) and ^{7}Li(^{6}Li,^{7}Be,t) at 455 MeV beam energy, explained as a SDM resonance structure, while enhancement above 24 MeV (α-core break-up point) explained as observation of GDR in the α – cluster of parent nuclei [14]. Obviously there is a problem of not observing the narrow structures in these experiments. There are three possible explanations:

- These experiments are not providing the data for kinematically complete analysis of ^{6}He→tt decay as compared to the data of Ref. [15, 19]. The final state of the reaction ^{7}Li(^{6}Li,^{7}Be,t)X can not be only ^{6}He*, decaying into tt channel, but also contribution of ^{7}Li(^{6}Li, ^{4}H*dn) reaction with E_x threshold quite close to that for ^{6}He→tt one as well as contribution of excited ^{6}He* decay into ^{4}H*+d, ^{4}H+d or t+p+d channels.
- The possible excitation of ^{7}Be fragment can also be non-vanishing. In Ref. [18], for example, a 0.45 MeV Doppler-shifted photon has been registered, produced by first level de-excitation of ^{7}Be nuclei, used for energy correction and spin determination purposes. These contributions, may smear the resonance structures in kinematics reconstruction and increase the total background.
- The use of relatively heavy projectiles or high energy beam allows the high spin transfer to the reaction fragments, that is in principle useless for search of low spin resonance excitations but may enrich the resonant and phase-space background contributions.

By selecting the final states, consisting of registered clusters and non-registered nucleons, the complete kinematics reconstruction is becoming possible and physical background decreases as compared to the scheme with not registered cluster and its fragments, leading to the additional contribution of four particle final state.

In conclusion to this part, the results of many presented experimental works suffer of non-complete kinematics analysis and high background conditions.

3.1. Scheme of experimental setup

The scheme of the experimental layout in the horizontal zx-plane is shown in Fig.1a.

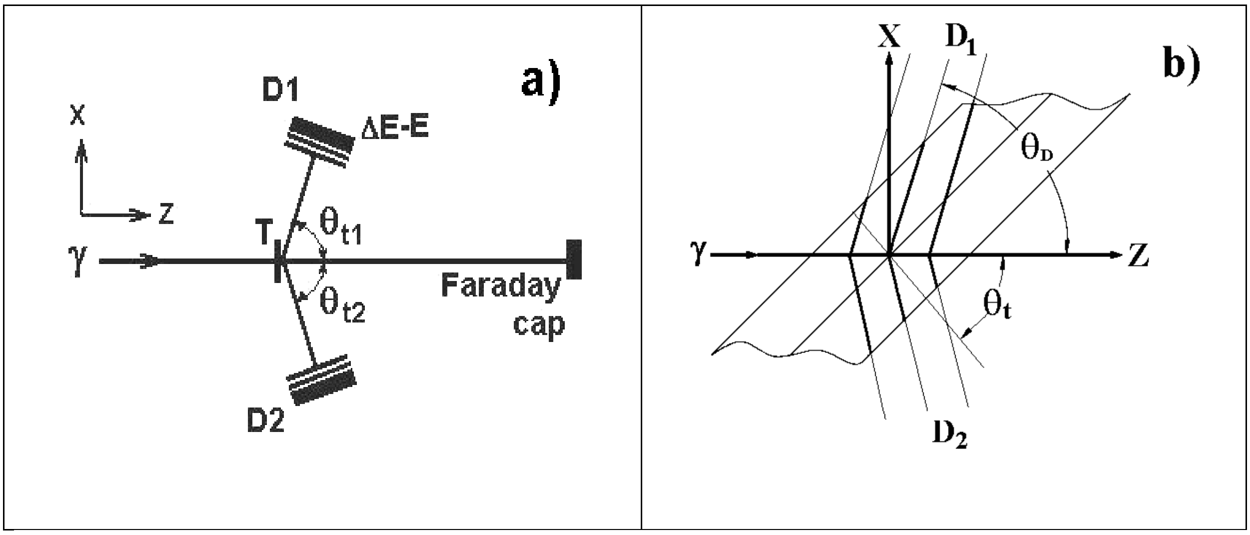

Fig.1: a) The layout of the experimental setup; b) the alignment of the lithium target.

The concept of a two-arm set-up of Si-detector telescopes [24] with a sensitive area of (100x100) mm^2 for registration of two tritons in coincidence has been chosen. Geometrically the telescopes are located at a distance of 20 cm from the target covering a solid angle of 0.25 sr each. Both telescopes consist of two perpendicular arrays of 50 μ thick dE/dx silicon sensors of 5 or 10 mm strips size and a 1.5 mm thick E-detector with an energy resolution of app.1%, that allows to identify the particles, measure their kinetic energy in the range of 4-20 MeV and reconstruct the triton angles. The photon beam will be generated by the bremsstrahlung of the 75 MeV electron beam of Yerevan Electron Synchrotron, working in low energy stretcher mode with the expected intensity above 10^{10} photons/s. Enriched (99%), 150-200 μ–thick metallic lithium foils will be used. The beam spot size on the target is expected to be less than (10x10) mm^2. The target holder and detectors will be mounted in a vacuum chamber. The special target alignment (see Fig.1b) is discussed in section 3.2.2.

3.2. Monte Carlo simulation

To work with kinematic distributions and determine the necessary requirements to the performance of the experimental set-up the Monte-Carlo simulations were carried out.
Event generation is done by a Fortran-based GENBOD code [25]. It generates the event of out-going multi-particle momentum vectors in the centre of mass according to the Lorentz-invariant Fermi phase space.
The total centre of mass energy as well as the masses of the outgoing particles are specified in the user package. GENBOD gives the weight which must be associated with event according to physics requirement. To include the resonances in binary system the Breit-Wigner distribution of the weights has been assumed for the invariant mass of two particles. The user package also includes the beam-line and experimental setup simulation as well as the kinematical reconstruction and data analysis codes. The beam line simulation includes the bremsstrahlung energy spectrum and beam special distribution in xy-plane (Fig.1a). The target simulation includes an alignment description, the distribution of photon hits, as well as the ionisation losses and multiple Coulomb scattering. The detectors simulation part contains

the geometry description, the hits coordinates calculation in Si-detectors, ionisation losses, ranges and corresponding energies deposit in the telescopes as well as their smearing due to the energy resolution. Details of kinematical reconstruction analyses are given in sections 3.2.2 and 3.3.

The kinematical distributions have been generated for the following processes:

- three-body disintegration process (1) - $\gamma + {}^7Li \rightarrow t + t + p$
- quasi-two-body disintegration process (2) - $\gamma + {}^7Li \rightarrow {}^6He^* + p$ with subsequent decay of excited $^6He^*$ states ($^6He^* \rightarrow t+t$), and
- quasi-two-body disintegration process (3) - $\gamma + {}^7Li \rightarrow {}^4He^* + t$ with subsequent decay of excited $^4He^*$ states ($^4He^* \rightarrow t + p$)

As it was mentioned above, the phase-space process (1) represents a general background for the resonance excitation channels, but the process (3) can contribute as a background to the process (2) as well, so the detector configuration should provide a maximal separation of the kinematic distributions of the processes (2) and (3) .

The experimental data of reference [19] on the ^6He levels were used for Monte-Carlo simulation allowing to scan the excitation energy range E_x=10-40 MeV (Table 2).

Table 2. Excitation energy levels of ^6He used for simulation [19]

E_x , Γ	Levels notation
15.8±0.6 MeV; 1.1±0.6 MeV	A
20.9±0.3 MeV; 3.2±1.5 MeV	B
31.1±1.0 MeV; 6.9±2.3 MeV	C

There is practically no cross-section data on the process (2) for ^6He excitation energy above 10MeV, the available ones are not reliable and mostly based on the inclusive or semi-inclusive measurements of the proton or triton yield and thus have not been involved in Monte-Carlo simulations. The possible similarity of the cross-sections in the process (2) and $\gamma + {}^7Li \rightarrow {}^6He(g.s.) + p$ [26], is exploited in yield evaluation only.

3.2.1 Detector configuration setting

The set of kinematic distributions of the process (2) was simulated with invariant mass M_{12} of two tritons compatible with excitation energies of $^6He^*$, defined as $E_x = M_{12} - M_{6He}$, where M_{6He} is the mass of ^6He ground state and M_{12} can be expressed through the measured kinematical parameters of the tritons as follows:

$$M_{12} = \sqrt{4M_t^2 + 2M_t\left[(T1+T2) - \sqrt{2(T1 \times T2)} \times \cos(\vartheta_{12})\right] + 2T1 \times T2}. \qquad (1)$$

where M_t, $T1$, $T2$ are the triton mass and kinetic energies and ϑ_{12} is the angle between the tritons momenta.

Although the detector registration efficiency for the process (2) certainly depends on the excitation energy of interest, the energy range E_x =10–60 MeV can be covered by two setting of telescopes, optimized for energies E_x = 20.9 and 31.1 MeV.

The detector configuration has to provide a compromise between the maximal registration efficiency of process (2) and its kinematical separation from the process (3). For this purpose the telescopes have been set at a non-coplanar configuration ($\varphi_1 - \varphi_2 < 180^o$) that suppresses rather coplanar angular distribution of the tritons from the process (3) as compared to the process (2) (see Fig.2a and insert there). The details of numerical evaluations are presented in section 3.3.

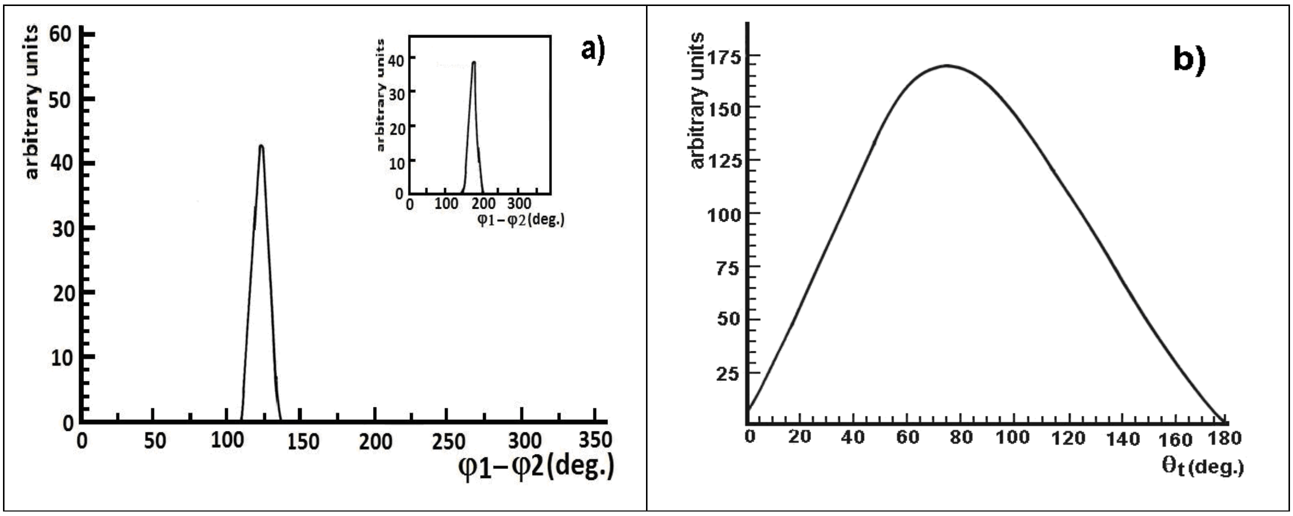

Fig.2: a) The distribution of tritons azimuthal angle difference ($\varphi_1 - \varphi_2$) in the process ^{7}Li(γ,^{6}He*)p and ^{7}Li(γ,^{4}He*)t in the insert; b) the tritons (t1,t2) polar angle distribution in the process ^{7}Li(γ,^{6}He*)p.

Having the azimuthal angles fixed, the choice of tritons' polar (θ_{t1},θ_{t2}) proceeds through simulation of the process (2) at fixed photon and excitation energies without limitation on the detector aperture. The Fig.2b shows the distributions of polar angles for the process (2) at E_γ = 50 MeV. The telescopes have been installed according to the peak positions in these distributions, allowing to reach the maximal registration efficiency.

The detector configuration parameters: the average polar and azimuthal angles and kinetic energies of the tritons and proton, adopted to "B" and "C" levels excitation are shown in Table 3.

Table 3. Setup configuration parameters

Configuration	$E_x \pm \Gamma/2$ (MeV)	$<\theta_{t1}>$ (deg)	$<\theta_{t2}>$ (deg)	$<\varphi_1-\varphi_2>$ (deg)	$<T_{t1,t2}>$ (MeV)	$<\theta_p^{cm}>$ (deg)	$<T_p>$ (MeV)
1	**20.9±1.6**	**83**	**83**	**120**	**5.7**	**82**	**15.7**
2	**31.1±3.5**	**87**	**87**	**150**	**9.9**	**77**	**8.1**

(*) Except θ_p^{cm}, the data are given in the laboratory system.

As one can see from Table 3, the telescopes are installed symmetrically with respect to the photon momentum, they have the same polar angle, but are not co-planar due to proton recoil.

3.2.2. Kinematics reconstruction and experimental resolutions calculation

The complete three-body kinematics, including photon and excitation energies E_γ and E_x, was reconstructed using the six measured parameters: the triton angles and momenta. The reconstruction proceeds trough the angles reconstruction using the Si-pixel hits and assuming the point-like target. During the reconstruction, the average ionization energy losses in the target for the energy of each registered triton are calculated and added to the energy response measured by telescopes. This procedure preserves an appearance of the systematic shift in reconstructed photon and excitation energies. However, apart of the average energy losses in the target, the triton ranges are varying around their average that causes a visible worsening in the excitation and photon energy resolutions. This contribution can be in principle reduced by appropriate target alignment relative to a beam direction, providing correlated and relatively weak variation of summary range of two tritons versus photon interaction depth. The kinematical effect of the alignment may be understood from the expression for invariant mass M_{12} (section 3.2.1), while it can be simply understood by a target alignment sketch in the case of telescopes co-planarity, shown in Fig.1b. Single rotation in the reaction plane ($\theta_t = 45^o$ - $(90^o - \theta_D)$) is needed in this case to achieve the necessary alignment. In non-coplanar geometry the optimal alignment can be achieved by two successive rotations. The effect of alignment, however is most effective for the telescopes polar angles close to 90^o and reduces to zero at 45^o. The contribution of the experimental uncertainties such as the granularity and energy resolution of detectors, beam spot size, multiple scattering and ionization energy losses in Li target on the photon and excitation energy resolutions have been simulated and investigated separately, and the results are shown in Table 3 for the particular case of the detector setting optimized for “B” level. The expected experimental resolutions can be determined by comparing the true kinematical parameters of the particles with ones obtained after chain of simulation and reconstruction.

Table 4. Contributions of experimental uncertainties into the energy resolutions for configuration “1”

	Multiple scattering in target	**Uncertainties of ionization losses in target**	**Beam spot size in target (10x10)mm^2**	**Detector granularity (10x10)mm^2**	**Detectors energy resolution**	**All factors together**
σ_{Ex} (MeV)	0.08	0.19	0.21	0.23	0.08	0.38
$\sigma_{E\gamma}$ (MeV)	0.47	0.28	1.22	1.28	0.08	1.71

As one can see from Table 4, the main contribution to the excitation and photon energy resolution is coming from the ionization losses, beam spot size, detector granularity and less from the multiple scattering and detector energy resolution. Account of all the experimental uncertainties gives quite acceptable result as compared to widths of the energy levels “A” and ”B”. The change of the detector granularity from (10x10)mm^2 to (5x5)mm^2 improves the excitation and photon energy resolutions by 10% only, as might be expected from the data of Table 4. The excitation energy resolution has been calculated in the energy range of 10-40 MeV for both detector configurations, ”1” and ”2” and it runs from app. 0.23 MeV at the bottom to a 0.7 MeV at the top end of this energy range.

3.3. The simulation results

The invariant mass distribution of two tritons for the processes (2) with excitation energies of ^{6}He above 15.8 MeV are plotted in Fig.3a and Fig.3b for detector configurations “1” and “2”.

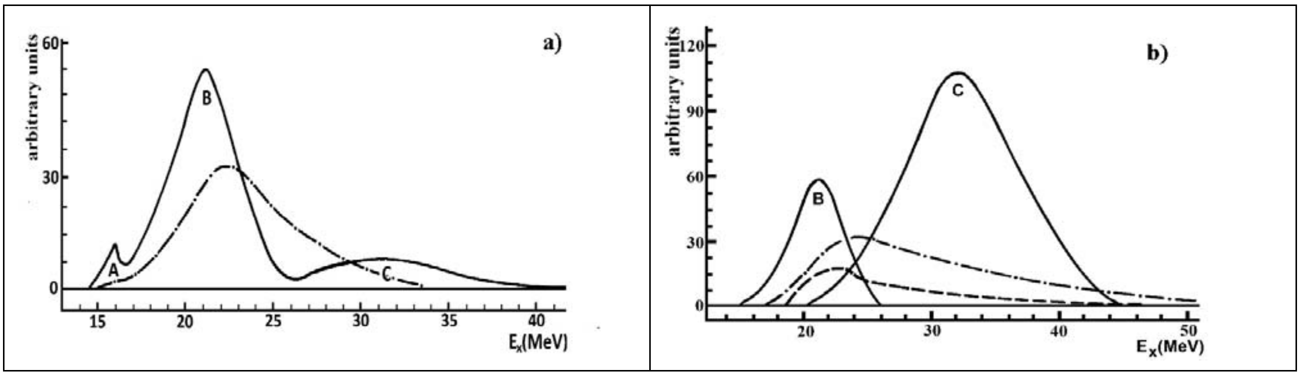

Fig.3: a) The simulated invariant mass distribution of two tritons for the process ^{7}Li(γ,^{6}He*)p at three resonance energies (“A”,”B”,”C”) in the detector configuration “1”(solid line) and phase-space one (dot-dashed line); b) the same for resonance energies (”B”,”C”) in the detector configuration “2”. Shown by dashed line is the contribution of the process ^{7}Li(γ,^{4}He*t).

Superimposed in the figures are the contributions of the phase-space process (1) as well as not negligible contribution of the process (3) in Fig.3b.

The yields of the process (2) and (3) in the figures are consistent with the rate evaluations. The contribution of ^{6}He excitation at 15.8 MeV is absent in the detector configuration “2”, which is explained by its strong kinematic suppression. However in configuration "1" its yield is also small due to low tritons energy to be registered. The yield of the process (2) at excitation energy 20.9 MeV is relatively stable in both detector configurations ”1” and “2”, which are in average more sensitive to the lower and higher energy parts of the acceptable excitation energy range respectively. Fig.4a,b and Fig.5a,b show the energy spectra of the registered tritons and corresponding photons in two detector configurations “1” and ”2” at given three excitation energies, allowing to see and evaluate the peculiarities of expected experimental distributions.

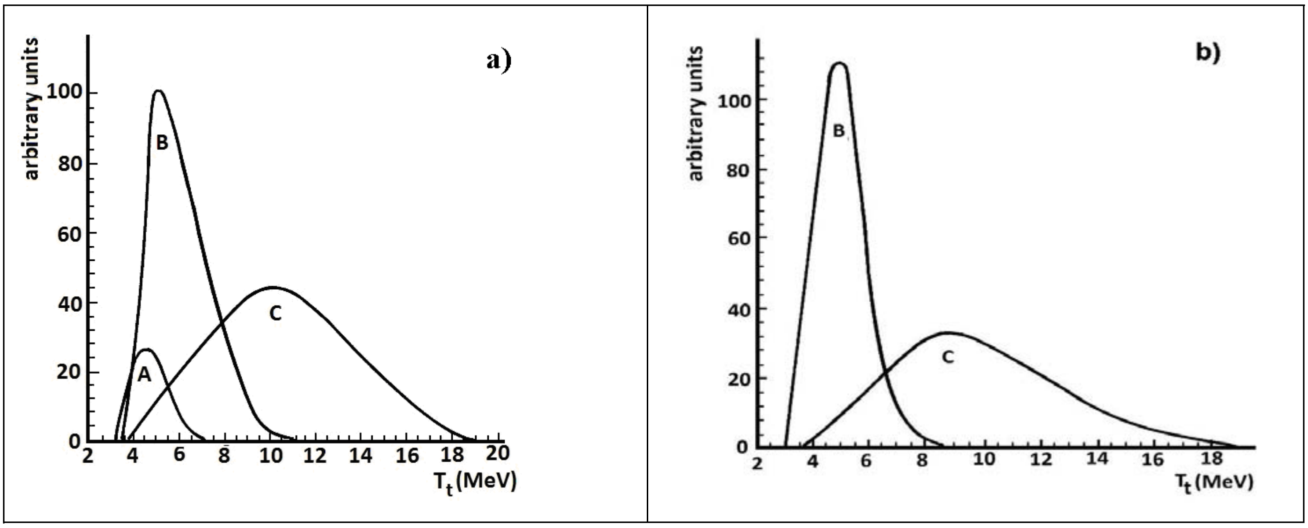

Fig.4: a) The tritons spectra simulated for the process ^{7}Li(γ,^{6}He*)p at three resonance energies (“A”,”B”,”C”) in the detector configuration “1”; b) the same at resonance energies (”B”,”C”) in the detector configuration “2”.

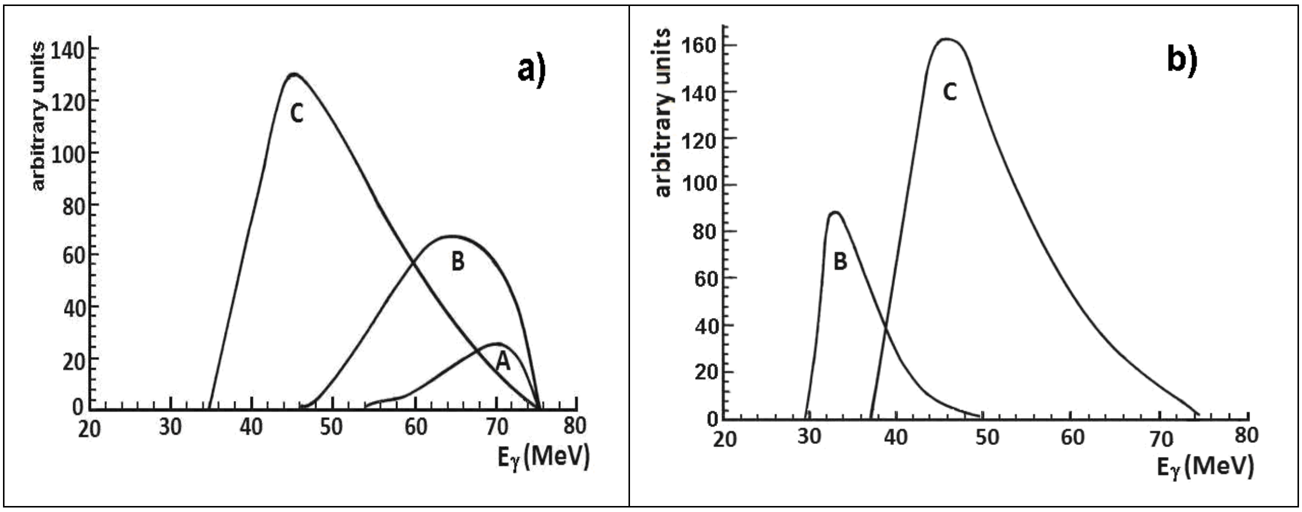

Fig.5: a) The photons energy spectra simulated for the process ^{7}Li(γ,^{6}He*)p at three resonance energies (“A”,”B”,”C”) in the detector configuration “1”; b) the same at resonance energies (”B”,”C”) in the detector configuration “2”.

As one can see from Fig.5a the incident photon spectrum is becoming harder with excitation energy decrease in detector configuration “1” that can be seemed surprising. However, the triton kinetic energy (Fig.4a) is composed from the share of the parent nuclei recoil, correlated with photon energy and excitation energy, that is smallest for level ”A”, so only the most energetic photons provide enough energy for the tritons to be registered. This in general explains the structure of γ-spectra observed in Fig.5a. The detector configuration “2” provides more kinetic energy to tritons and less to protons (see Table 3) that explains the γ-spectra observed in Fig.5b.

- The yield of the phase-space process (1) in Fig.3a,b is shown in arbitrary units. According to the observations (see [27] and references therein) and theoretical investigations [28], the mechanism of system’s break-up to a three-body final state is prevailed by a sequential decay through the resonances in the binary systems if they have a width smaller than the excitation energy. As it is indeed the case of narrow resonances, one can expect that the phase space contribution will be suppressed in the spectra of invariant mass distribution. This statement is consistent with the experimental data [15, 19].
- The expected rate of the process (2) for the ^{6}He excitation at energies E_x =15.8(A), 20.9(B) and 31.1 MeV(C) have been evaluated using the experimental data on the process ^{7}Li(γ,p)^{6}He(g.s.) [26], obtained for the photon energy range 50-120 MeV and θ_p^{cm} =24-144^o, assuming the same level of the yields for the ground and excited states of ^{6}He that is certainly indicated by the experimental data [23]. The polar angle distribution for the process (2) in CM system is quite wide, in particular $\theta_p^{cm} = 82^o \pm 18^o / 77^o \pm 25^o$ for the detector configuration “1” and “2”. The differential cross-sections averaged over the angular and photon energy range accepted for the experimental setup have been evaluated to be in the order of 1-3 μb/sr at effective photon energy range E_γ = 50-70MeV, corresponding to the excitation energy range 15-31 MeV.

The yield of the process (2) can be calculated according to the standard definition $N_{evt} = N_t * N_\gamma * \langle d\sigma/d\Omega\rangle * \Delta\Omega * \varepsilon$, where $\langle d\sigma/d\Omega\rangle$ and $\Delta\Omega$ are the cross-section and simulated proton solid angle in the CM system, while N_t, N_γ, and ε denote the nuclei density in the target, photon intensity in the acceptance of the setup, and efficiency of registration, that accounts for the detector geometry and particle losses in the target and detector. The efficiency is defined by Monte-Carlo simulation as the ratio of the registered events to the generated ones for the selected range of excitation energy and proton CM angles. The efficiency strongly varies, depending on the excitation energy and detector configuration, increasing from $5{*}10^{-5}$ at E_x=15.8 MeV to $7{*}10^{-4}$ at 20.9 MeV and $6{*}10^{-3}$ at 31.1 MeV, partly due to hardening of the tritons’ energy spectra. In particular, at excitation energy E_x=15.8 MeV it is too soft and partly below the threshold of 3.5-4 MeV, needed to be registered in successive layers of Si-pixels (see tritons spectra in Fig.4a and 4b).

For the realistic values of N_t and N_γ to be in the order of 10^{21}cm^{-2} and 10^8s^{-1}, respectively, one can expect a maximal event rate of the order of 0.2 event/h, 7.2 event/h and 32event/h for the energy levels “A”,”B” and “C”, respectively.

- The rate evaluation for the process $\gamma + {}^7\mathrm{Li} \rightarrow {}^4\mathrm{He}^* + t$, using the cross-sections data [29] is performed similarly to the process (2), assuming the same magnitude of the differential cross-sections for the ground and excited states of ^{4}He in the photon energy range E_γ= 50-75 MeV. The excitation of ^{4}He levels above E_x=20 MeV [20] of the ground state is simulated. The telescopes non-co-planarity alone provides app. two order of magnitude suppression of the process (3) in configuration “1” as compared to the process (2) at excitation energy “B”, while in configuration “2” this suppression is one order of magnitude only (level ”C”). The shape of (tt) invariant mass distribution in the process (3) (Fig.3b) is quite smooth and similar to that of the process (1), so it seems that the background contribution in configuration “2” would be acceptable for the statistically reliable process (2) separation. Additional kinematical separation of the process (3) contribution is also possible. For example, Fig. 6 shows the proton energy spectra in the processes (3) and (2) at E_x=31.1 MeV, allowing to see the possibility of simple cut, giving a factor three decrease of the process (3) contribution into the process (2).

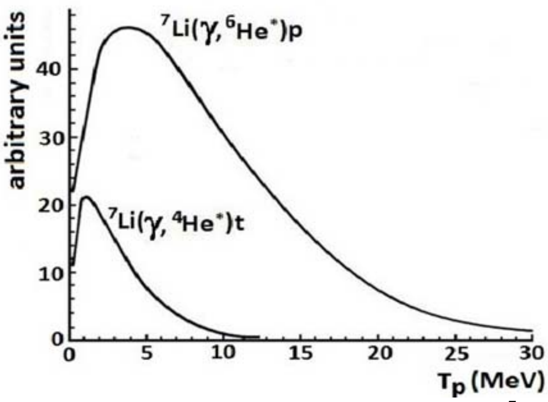

Fig.6: The proton energy spectra (laboratory system) for the processes ^{7}Li(γ,^{6}He*)p and ^{7}Li(γ,^{4}He*)t at excitation energy "C" in (tt) system.

- The analysis of data shown in Fig.3a and Fig.3b will be done with assumption of a smooth polynomial fit to the invariant mass M(1,2) of two tritons in the phase space distribution and Breit-Wigner shapes for the levels excitations. The description of phase-space background, not affected by the resonance structures is a subject of the separate study; in particular it might be built combinatorially, composed of the triton 1 and triton 2 kinematic parameters from different events.
- The analysis of γ -spectra in the reactions $\gamma + {}^7\text{Li} \rightarrow {}^6\text{He}^* + p$ ($^6\text{He}^* \rightarrow t+t$) and $\gamma + {}^7\text{Li} \rightarrow t+t+p$ may allow to observe two types of excited states of $^7\text{Li}^*$ nucleus like $({}^6\text{He}^* + p)^*$ and $(t+t+p)^*$ and determine the excitation energy $E_{x,}$ related to certain E_γ values of the bremsstrahlung γ spectrum.
- Another important subject of the experimental method is the separation of the accidental background in t+t events produced by different photons within the time gate of registration. With aim to study and remove these contributions, a time-of-flight analysis of the signals registered in two arms can be done. The distribution of the time-of-flight difference measured and reconstructed between two arms of the telescopes can be written as $\delta t = (t1\text{-}t2)^{meas} - (t1\text{-}t2)^{reco}$. The reconstruction is based on the knowledge of the measured kinetic energies and time-of-flight distances for the heated detection bins. The true differences are concentrated around $\delta t = 0$ within the width of 1.45ns, consistent with experimental uncertainties of Table 3, while for the accidentals, this distribution must be flat, as the stretcher beam has no bunch structure that allows a simple fit of background and easy separation of true process (2) events (see section 3.2).

4. Conclusions

We propose to explore the three body break-up of the light nuclei using ^{6}Li, ^{7}Li and ^{9}Be targets in seven photo-disintegration reactions with purpose of investigating the cluster structures of 24 excited states of seven isotopes: ^{5}He, ^{6}He, ^{5}Li, ^{6}Li, ^{7}Li, ^{8}Be, ^{9}Be.
As an example, the excitation of ^{6}He nucleus is simulated in photo-disintegration reaction $\gamma + {}^7\text{Li} \rightarrow {}^6\text{He}^*(t+t) + p$ using two-arm setup of Si-strip telescopes. The physical background, including three body phase space $\gamma + {}^7\text{Li} \rightarrow t+t+p$ and $\gamma + {}^7\text{Li} \rightarrow {}^4\text{He}^*(t+p) + t$ reactions was also simulated and possible contribution analysed. The proposed experimental method has an advantage of complete reconstruction of three-body final state kinematics without detection of the third particle (nucleon). As a result the feasibility of the experimental study of the reaction $\gamma + {}^7\text{Li} \rightarrow {}^6\text{He}^*(t+t) + p$ is demonstrated, both on experimental resolutions for excitation and photon energies, allowing to resolve and identify the energy levels of ^{6}He nuclei, as well as on the expected luminosity. According to the yield evaluations, the 250-300 hours of the beam time would be enough to observe and analyse the excitation of ^{6}He levels in the energy range E_x=10-40 MeV. The same experimental program, with minor variations, might be also applied to the list of the photo-disintegration reactions presented in section 2.

References

[1] **M.Kimura, N.Furutachi, Y.Taniguchi ,Y.Kanada-En'yo and H. Horiuchi**, Clustering Aspects of Highly Excited States and Neutron-Rich Nuclei. Progress of Theoretical Physics Supplement No. 196, 2012

- **C.Beck, P.Papka, A.Sànchez et al.**, Clusters in Light Nuclei, Acta Physica Polonica **B42** No 3– 4, 2011
- **K.Ikeda et al.**, Clusters in Nuclei, vol.1, Lecture Notes Phys. **818**, p.165, ed. C. Beck, 2010
- **M.Ito, N.Itagaki, and K.Ikeda**, Cluster correlations for low-lying intruder state of ^{12}Be, Phys. Rev. **C 85**, 014302, 2012
- **D.M.Brink**, History of cluster structure in nuclei. Journal of Physics: Conference Series 111 012001, 2008

[2] **T.Yamada et al.**, in Clusters in Nuclei, Lecture Notes in Physics, edited by C. Beck, **Vol. 2** (Springer-Verlag, Berlin, 2010)

[3] **E.Epelbaum, H.Krebs, Timo A.Lahde, D.Lee, and Ulf-G. Meißner**, Structure and Rotations of the Hoyle State, Phys. Rev. Lett. **109**, 252501, 2012

[4] **M.Gai et al.**, The structure of ^{12}C and Stellar helium burning in γ induced ^{12}C dissociation, Acta Phys. Pol. **B 42**, 775, 2011

[5] **R.M.Itoh et al.**, Candidate for the 2+ excited Hoyle state at $E_x \approx$10 MeV in ^{12}C, Phys. Rev. **C 84**, 054308, 2011

[6] **T.K.Rana, S.Bhattacharya, C.Bhattacharya et al**, Direct observation of the decay of first excited Hoyle state in ^{12}C, arXiv:1203.3336v1 [nuc-ex] 15 March 2012

[7] **F.D.Smit, F.Nemulodi,1, Z.Buthelezi, et al.**, No evidence of an 11.16 MeV 2+ state in ^{12}C, arXiv:1206.4217v1 [nucl-ex] 19 June 2012

[8] **A.N.Kuchera, G.V.Rogachev, V.Z.Goldberg, et al.**, Molecular structures in T = 1 states of ^{10}B, Phys. Rev. **C 84**, 054615, 2011

[9] **G.Hansen and B.Jonson**, Europhys. Lett. **4**, 409, 1987

[10] **A.S.Fomichev, V.Chudoba, I.A.Egorova et al.**, Phys.Letters **B 708** p.6, 2012

[11] **H.Akimune, T.Yamagata, S.Nakayama et al.**, Trinucleon Cluster Structure at High-Excitation Energies in A = 6, Nucl. Phys. Rev. **C 67**, 051302 (R), 2003
T.Yamagata, H.Akimune, Nakayama et al., Di-trinucleon cluster resonances in A= 6 isobar nuclei, Phys. Rev. **C 71**, 064316, 2005

[12] **R.A.Eramzhyan, B.S.Ishkhanov, I.M.Kapitonov, and V.G.Neudachin**, The Giant Dipole Resonance in Light Nuclei and related phenomena, Physics Reports **136**, No. 46 229-400, 1986

[13]**Б.С.Ишханов, И.М.Капитонов**, ГДР в атомных ядрах, (http://nuclphys.sinp.msu.ru/gdr/), 2009

[14]**S.Nakayama, T.Yamagata, E.Matsumoto et al.**, Phys. Rev. **C78**, 014303, 2008 **T.Yamagata, H. Akimune, S. Nakayama et al.**, Phys. Rev. **C 77**, 021303 (R), 2008.

[15]**O.M.Povoroznyk, O.K.Gorpinich, O.O.Jachmenjov, H.V.Mokhnach, O.Ponkratenko, G. Mandaglio, F. Curciarello, V. De Leo, G. Fazio and G. Giardina**. Phys. Rev. **C 85**, 064330, 2012.

[16] **P.Brady, N.S.King, B.E.Bonner, et al.**, Phys. Rev. **C 16**, 31, 1977

[17] **S.B.Sakuta, B.G.Novatsky, D.N.Stepanov et al.,** Physics of Atomic Nuclei, **65**, No. 10, pp. 1771–1777, 2002. Translated from Yadernaya Fizika, **65**, No. 10, pp. 1819–1825, 2002

[18] **J.Jannneke, T.Annakkage, G.P.A.Berg, et al**., Phys. Rev. **C64**,1070, 1996

[19] **Ю. Гуров, В.С Карпухин, С.В.Лапушкин и др.**, Письма в ЖЭТФ, **84**, с.3-7, 2006

[20] http://www.nndc.bnl.gov/ensdf/

[21] **D.Tilley et al.**, Nucl. Phys. **A708**, p.3-163, 2002
F. Ajzenberg-Selove, Nucl. Phys. **A490**, 1, 1988

[22] **N.Demekhina et al.**, e-Print: arXiv:0909.1630 [nucl-ex], 2009 and e-Print: arXiv:1106.1582 [nucl-ex], 2011.

[23] **M.J.Boland et al.,** Phys. Rev. **C64**, 031601-1, 2001

L.Lapikas,J.Wesseling and B.Wiringa, Phys.Rev.Lett. **82**, 4404, 1999
[24] Research Institute of Material Sience and Technology, Zelenograd, Russia http://www.niimv.ru/
[25] CERNLIB: FOWL (W505), GENBOD (W515)
[26] **M.R.Sene et al.**, Nucl. Phys. **A442**, p.215, 1985
S**. N. Gardner et al.**, Phys. Lett. **46B**, p.186, 1973
[27]Thesis for the degree of Doctor of Philosophy, Aarhus University, http://www.phys.au.dk/fileadmin/site_files/publikationer/phd/Hans_Fynbo.pdf
[28] **A.A.Korsheninnikov**, Sov. J. Nucl. Phys.**52**, 827, 1990
[29] **Burkova N.A, Denyak V.V, et al.,** *Nucl. Phys.***A586**, 293, 1995